Phytopathology Research

RESEARCH

Open Access

The b-ZIP transcription factor, FgBzip16, is essential for fungal development, ascospore discharge, and pathogenicity by modulating fatty acid metabolism in *Fusarium graminearum*

Bing Li[1,2,3†], Yuhe Shen[2†], Yupan Zhu[2], Lingling Yang[2], Ruonan Ma[2], Hao Sun[2], Jingang Liang[4], Kangkang Chen[1], Zhen Jiao[2*] and Wenchao Yang[1*]

Abstract

Fusarium graminearum is an economically devastating pathogen that causes cereal worldwide. The plant disease cycle involves sexual reproduction, with the perithecium playing a crucial role in overwintering and the discharge of ascospores. Although fatty acid biosynthesis and metabolism are linked to perithecium formation and ascospore discharge, the regulation of these processes remains largely unknown. In this study, we identified and characterized *FgBZIP16*, as a basic leucine zipper (b-ZIP) transcription factor, in *F. graminearum*. Targeted gene deletion revealed that FgBzip16 is important for vegetative growth, asexual/sexual development, and plant infection. Cytological observations revealed that FgBzip16 was localized in the nucleus during the hyphal and conidial stages. FgBzip16 is essential for ascospore discharge, with transcriptomics and molecular biology showing it binds to the promoter of its target genes *FGSG_05321* and *FGSG_03244*, which regulate ascospore discharge by encoding fatty acid synthase subunit alpha-reductase and enoyl hydratase, respectively. Altogether, these results constitute the first report of the specific functions associated with b-ZIP transcription factor FgBzip16, linking its regulatory roles to fungal development, fatty acid accumulation, and metabolism, host penetration, and pathogenicity of *F. graminearum*.

Keywords b-ZIP transcription factor FgBzip16, Development, Ascospore discharge, Fatty acid metabolism, Pathogenicity

Background

Fusarium head blight (FHB), caused by the filamentous ascomycete *Fusarium graminearum*, is one of the most important diseases affecting major cereal crops, especially wheat (Bai and Shaner 2004; Goswami and Kistler 2004). Apart from causing significant yield losses, *F. graminearum* produces mycotoxins like deoxynivalenol (DON) and zearalenone (ZEA) that pose a threat to human and animal health (Proctor et al. 1995; Goswami and Kistler 2004; Audenaert et al. 2013). In the recurrent disease cycle of FHB, ascospores (sexual spores) and conidia (asexual spores) are primary and secondary inocula for plant infections caused by *F. graminearum*,

†Bing Li, Yuhe Shen contributed equally to this work.

*Correspondence:
Zhen Jiao
jiaozhen@zzu.edu.cn
Wenchao Yang
wenchaoyn@yzu.edu.cn
[1] School of Plant Protection, Yangzhou University, Yangzhou 225009, China
[2] School of Agricultural Sciences, Zhengzhou University, Zhengzhou 450001, China
[3] State Key Laboratory for Biology of Plant Disease and Insect Pests, Beijing 100193, China
[4] Development Center of Science and Technology, Ministry of Agriculture and Rural Affairs, Beijing 100176, China

respectively (Guenther and Trail 2005; Trail 2007). During suitable environmental conditions, ascospore production and discharge from the perithecium (sexual fruiting body) play essential roles in the spread of FHB (Bai and Shaner 2004). After the ascospores are discharged, the rapid germination of ascospores enables *F. graminearum* to infect wheat tissues. DON, an important virulence factor, promotes the spread of *F. graminearum* in wheat (Jansen et al. 2005). Currently, controlling FHB is challenging due to the lack of effective fungicides (Paul et al. 2008). Deciphering the polygenic factors involved in sexual reproduction may facilitate the development of novel strategies for controlling FHB.

Sexual reproduction plays a crucial role in the disease cycle of *F. graminearum*, and ascospores serve as the primary source of inoculum for plant infection. As a homothallic fungus, sexual reproduction can occur without mating in *F. graminearum*. Upon karyogamy and meiosis, in the perithecium, croziers develop ascites (Cavinder et al. 2012), and the asci cells undergo meiosis and mitosis, ultimately leading to the production of eight ascospores. Under favorable environmental conditions, the ascospores are ejected or ooze out of the mature perithecia.

Fatty acid metabolism is believed to be a crucial resource for the formation of perithecium and the discharge of ascospores, which require large amounts of energy and precursor compounds (Cavinder et al. 2012). Lipid metabolism plays a vital role in the sexual development of fungi (Calvo et al. 2001; Hynes et al. 2008; Boisnard et al. 2009; Shin et al. 2020). A novel transcription factor, Fpo1, negatively regulates perithecial development in *F. graminearum* by reprogramming fatty acid metabolism, particularly fatty acid production, after sexual induction (Shin et al. 2020). Sexual development in *Podospora anserina* requires hydrolysis and consumption of fatty acids through peroxisomal β-oxidation and mitochondrial pathways (Boisnard et al. 2009). Furthermore, fatty acid utilization through peroxin (PEX) and glyoxylate cycle genes is crucial for sexual development in *F. graminearum* (Lee et al. 2009a, b; Min et al. 2012; Wang et al. 2008).

Transcription factors (TFs) are regulators that ensure the correct expression of target genes at the appropriate time and location, playing important roles in key cellular processes (Shelest 2008). Based on their DNA-binding domain types, most TFs can be classified into various classes, including basic region leucine zipper (b-ZIP), Myb, MADS-box, helix-loop-helix, homeobox and zinc fingers (Pabo et al. 1992). Previously, Son et al. (2011) constructed a 657 putative TFs mutant library and systematically analyzed 17 mutant phenotypes, among which 105 mutants exhibited altered sexual development. However, the regulatory mechanisms of sexual reproduction involving TFs remain largely unknown. Further investigation of these mechanisms may help in controlling FHB.

In this study, we identified and characterized FgBzip16, a b-ZIP TF that plays a crucial role in vegetative growth, asexual/sexual development, deoxynivalenol production, and plant infection. RNA-Seq analysis revealed that FgBzip16 regulates the expression of genes associated with fatty acid biosynthesis and metabolism. Further investigation demonstrated that FgBzip16 targets the fatty acid metabolism-related genes to control fatty acid metabolism. Overall, our study reports that FgBzip16 is essential for ascospore discharge and pathogenicity by modulating fatty acid biosynthesis and metabolism in *F. graminearum*.

Results

Identification of the *FgBZIP16* gene and examination of its expression

A BLASTP search against the protein sequence of Bzip16 from *Saccharomyces cerevisiae* identified an ortholog of B-zip16 (*FGSG_09832*) in *F. graminearum*. *FGSG_09832* was predicted to encode 297 amino acids and was named FgBzip16. Further domain analyses showed that FgBzip16 contains a typical b-Zip domain (152–219 aa) at the N-terminus (http://smartemblheidelberg.de/) (Additional file 1: Figure S1a).

To explore the FgBzip16 proteins, we first examined *FgBZIP16* transcription in different developmental stages using RT-qPCR. The results showed that *FgBZIP16* was expressed at all examined stages and had much higher expression levels in the conidia and perithecia, and during the early infection stage (Additional file 1: Figure S1b). Therefore, the *FgBZIP16* stage-specific expression pattern suggests that *FgBZIP16* plays an important role in the infection process and sexual reproduction of *F. graminearum.*

The *FgBZIP16* deletion mutant is defective in polarity growth and asexual development

To determine the function of *FgBZIP16* in *F. graminearum*, targeted gene deletion was performed using a split-marker strategy (Additional file 1: Figure S2a) (Li et al. 2019a). Putative mutants were identified by PCR screening and verified by Southern blot hybridization (Additional file 1: Figure S2b). Two independent Δ*Fgbzip16* mutants were obtained, both showing similar defective phenotypes. Therefore, one of the mutant strains was selected for further analysis. The mutant was complemented using the wild-type *FgBZIP16* gene with a GFP tag at the N-terminus, resulting in the restoration of all functions.

Firstly, the vegetative growth of the Δ*Fgbzip16* mutant was examined on CM and PDA agar plates. After 3 days of incubation, the colony sizes of the Δ*Fgbzip16* mutant were significantly lower than that of the wild-type strain PH-1 and the complementation strain (Fig. 1a and Table 1). Δ*Fgbzip16* produced highly branched, curled hyphae as compared to PH-1 (Fig. 1b). In 5-day CMC culture, Δ*Fgbzip16* was reduced in conidiation (Fig. 1c and Table 1) as the mutant produced 0.04×10^6 spores/mL compared to 1.28×10^6 spores/mL by PH-1 (Table 1). Moreover, more than 79.56% of the conidia produced by Δ*Fgbzip16* were abnormal (shorter in length, no more than three septa) comparison to those (< 18.73%) formed by PH-1 (Table 1). Additionally, we measured the

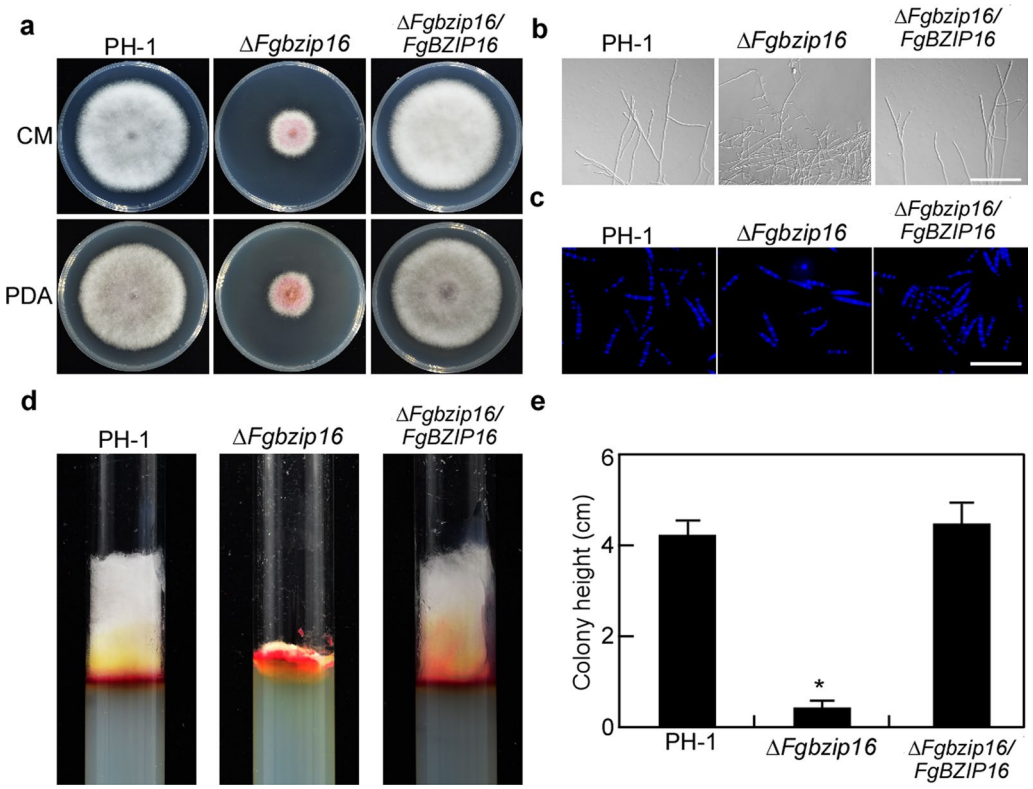

Fig. 1 FgBzip16 is important for polarity growth and asexual development. **a** The wild-type strain PH-1, Δ*Fgbzip16* mutant and complementation strain were cultured on CM and PDA medium at 25℃ for 3 days in the dark. **b** Hyphal branching of the indicated strains were grown on CM medium for 24 h. Bar = 10 μm. **c** Conidia of the indicated strains were harvested from CMC medium, stained with calcofluor white, and observed by fluorescence microscope. Bar = 10 μm. **d** Aerial hyphae of each strain in tubes cultured on potato dextrose agar. **e** Quantification of aerial hyphae from **d** in each strain. Line bars in each column denote the standard errors of three repeated experiments. The asterisks indicate a significant difference at $P < 0.01$

Table 1 Phenotypic analysis of the wild type strain PH-1, Δ*Fgbzip16* mutant, and complementation strain in *F. graminearum*

Strain	Colony diameter (cm)[a]		Conidiation	Conidial morphology(%)[c]		Conidial length
	CM	PDA	($\times10^6$ spores/mL)[b]	≥4 Septa	≤3 Septa	(μm)[d]
PH-1	7.1 ± 0.2	6.0 ± 0.3	1.28 ± 0.05	65.63 ± 2.35	33.18 ± 2.15	53.23 ± 3.13
Δ*Fgbzip16*	2.8 ± 0.3*	2.3 ± 0.1*	0.04 ± 0.01*	18.73 ± 1.24*	79.56 ± 1.83*	33.32 ± 2.17*
Fgbzip16/FgBZIP16	7.0 ± 0.1	6.1 ± 0.1	1.34 ± 0.08	63.12 ± 1.89	34.67 ± 3.65	50.87 ± 3.63

[a] Colony diameter of the indicated strains on different media after 3 days incubation at 25°C

[b] Quantification of the conidial production of the indicated strains from CMC cultures

[c] Percentage of the abnormal conidia of the indicated strains

[d] Measurement of the conidial length of the indicated strains

± SD was calculated from three repeated experiments and asterisks indicate statistically significant differences ($P < 0.01$)

proliferation of aerial hyphal heights, which showed that the hyphal heights of Δ*Fgbzip16* were lower than that PH-1 (Fig. 1d, e). Taken together, these phenotypes were consistent with the findings of a previous study (Son et al. 2011), indicating that FgBzip16 is required for vegetative growth, conidiation and conidial morphogenesis in *F. graminearum*.

The FgBzip16 is required for full virulence

To test whether FgBzip16 is required for *F. graminearum* pathogenicity, conidial suspensions of the PH-1, Δ*Fgbzip16* and complementation strains were inoculated onto flowering wheat heads at a concentration of 1×10^5 spores/mL. After 14 days of inoculation, Δ*Fgbzip16* did not cause head blight symptoms, while the PH-1 and complementation strains produced typical head blight symptoms (Fig. 2a). To gain further insight into the role of FgBzip16 during the expansion of invasive hyphae in the wheat head, a FgActin-RFP construct was created and used to transform PH-1 and the Δ*Fgbzip16* mutants. The resulting transformants were then inoculated onto flowering wheat heads.

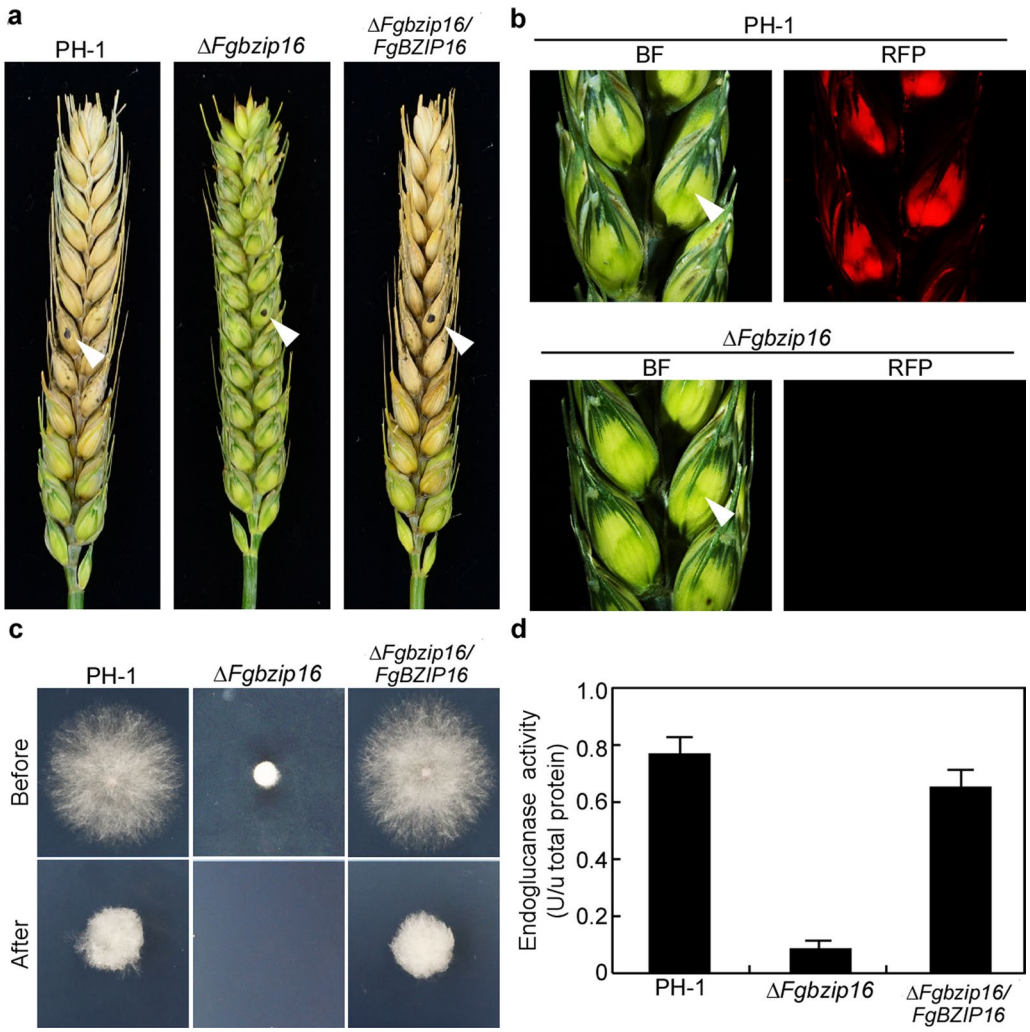

Fig. 2 Influence of *FgBZIP16* deletion on virulence and endoglucanase activity. **a** Flowering wheat heads were drop-inoculated with conidia of the wild type strain PH-1, Δ*Fgbzip16* mutant and complementation strain. Photographs were taken at 14 days post-inoculation (dpi). Inoculated spikelets were pointed by white arrows. **b** Spikelets were inoculated with conidia of each strain that expressed FgActin-RFP as control. Images were taken at 7 days. Inoculated spikelets were indicated by white arrows. **c** Penetration of cellophane by fungal hyphae. The strain was cultured on the top of cellophane membranes placed on minimal medium at 25°C. After 2 days of incubation, removed the fungal dishes and the cellophane membranes, and cultured the plates for an additional day and photographed. **d** Measurements of endoglucanase activity. The endoglucanase activity in mycelia was measured by spectrophotometrically. One unit of enzymatic activity is defined as 1 nmol/min reducing sugars released from the substrate. Line bars in each column denote the standard errors of three repeated experiments. The asterisks indicate a significant difference at $P<0.01$

Seven days post-inoculation, the RFP signal was limited to the inoculation site for the mutant, whereas it was prolonged in the wheat head for the wild-type strain (Fig. 2b). These results suggest that FgBzip16 plays an important role in the infection of wheat heads.

To further determine whether a defect in fungal penetration contributed to the Δ*Fgbzip16* mutant phenotype during infection, we performed the cellophane penetration assay, as previously described (Gu et al. 2015; Li et al. 2018). Δ*Fgbzip16* failed to penetrate the cellophane membrane, while the PH-1 and complementation strains successfully penetrated the cellophane (Fig. 2c). Consequently, we examined the endoglucanase activity as previously described (Jenczmionka et al. 2003). The endoglucanase activity in Δ*Fgbzip16* mutant was found to be decreased to 10% of that in PH-1 (Fig. 2d). These results indicated that the reduced endoglucanase activity contributed to the reduced fungal penetration and virulence of the Δ*Fgbzip16* mutant on wheat heads.

During *F. graminearum* infection, the mycotoxin DON is produced, and it is a virulence factor during the infection of wheat spike rachises (Proctor et al. 1995; Jansen et al. 2005). Therefore, we examined whether FgBzip16 regulated DON biosynthesis in *F. graminearum*. Compared with PH-1, the concentration of DON was not affected in Δ*Fgbzip16* (Additional file 1: Figure S3a). We further quantified the expression of two trichothecene biosynthesis genes, *TRI5* and *TRI6* (Seong et al. 2009) and found that the expression levels of two genes were not significantly different from those in PH-1 (Additional file 1: Figure S3b). This phenotype is consistent with the finding of a previous study (Son et al. 2011), indicating that FgBzip16 is not involved in the regulation of DON production in *F. graminearum*.

FgBzip16 is localized in the nucleus

FgBzip16 is a member of the b-zip family proteins of *F. graminearum*. We hypothesized that FgBzip16 is likely to be localized in the nucleus and shares the conserved cellular functions. To further decipher its functions, we examined its localization patterns in *F. graminearum*. We generated GFP-FgBzip16 and expressed it in the Δ*Fgbzip16* mutant. As mentioned previously, this construct rescued the mutant phenotypes. Large fluorescent spot structures were observed in the hyphal cells and conidia of Δ*Fgbzip16/FgBZIP16* (Fig. 3). We speculated that these structures were located in the nucleus. To test this hypothesis, we stained the hyphae with DAPI (4′, 6-diamidino-2-phenylindole: a nucleus marker) and examined whether it co-localized with GFP- FgBzip16. The results showed that GFP-FgBzip16 signals merged well with DAPI in the hyphae and conidia (Fig. 3). These results indicate that FgBzip16 is localized in the nucleus *F. graminearum*.

FgBzip16 is required for ascospore discharge in *F. graminearum*

As mentioned previously, sexual reproduction is an important step in the disease cycle of *F. graminearum* (Cavinder et al. 2012). It is a homothallic fungus. Therefore, we determined the sexual reproduction of PH-1 and Δ*Fgbzip16* on self-mating plates. After 10-day incubation, Δ*Fgbzip16* produced many perithecia and asci of normal size and morphology, which was similar to PH-1 (Fig. 4a). For ascospores release, after 24 h of incubation,

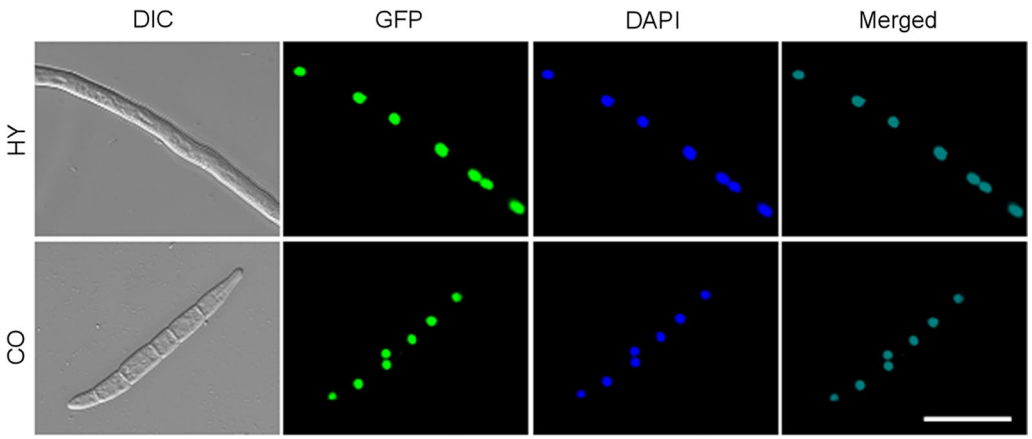

Fig. 3 FgBzip16 localizes to nucleus. Hyphae and conidia expressing the FgBzip16-GFP fusion construct were observed. DAPI (4′, 6-diamidino-2-phenylindole) staining of the nucleus at 25°C for 2 min. Photographs were examined under differential interference contrast (DIC) or epifluorescence microscopy. The merged panels showed the FgBzip16 localizes to nucleus. Bar = 10 μm

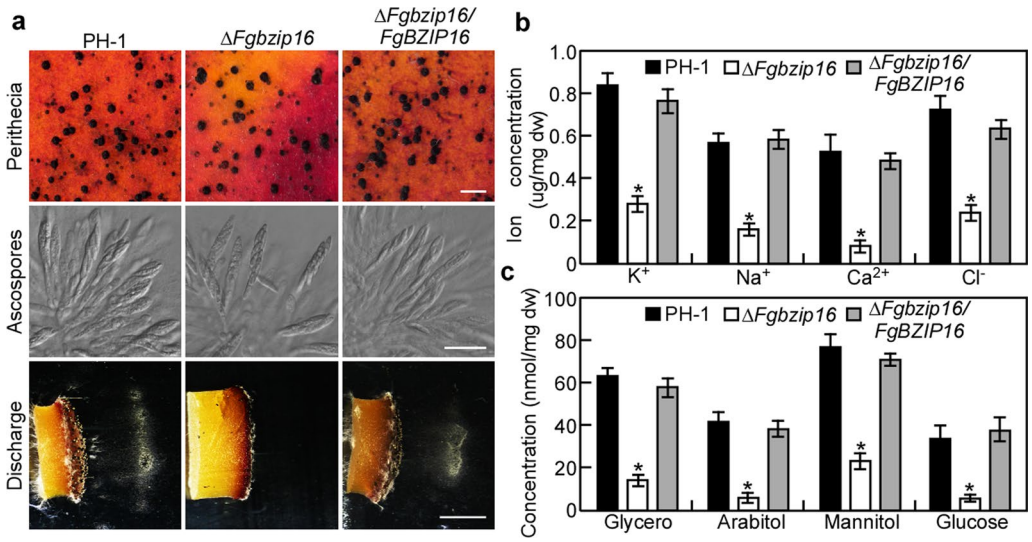

Fig. 4 FgBzip16 is essential for ascospore discharge, and for maintaining the normal concentration of ions and polyols in asci. **a** Perithecia, asci formation, and ascospore discharge of the indicated strains on carrot agar plates, and photographed at 10 days. Bars = 1 mm. The concentration of ions (**b**) and polyols (**c**) in the asci of the indicated strains, respectively. Line bars in each column denote the standard errors of three repeated experiments. The asterisks indicate a significant difference at $P < 0.01$

numerous ascospores were discharged from PH-1, while no ascospores were ejected from the perithecia of Δ*Fgbzip16* (Fig. 4a). These phenotypes were consistent with the findings of a previous study (Son et al. 2011), which showed that FgBzip16 plays an essential role in ascospore release in *F. graminearum*. The turgor pressure within the asci is generated by different ions and polyols and is responsible for ascospore discharge (Trail et al. 2002; Cavinder and Trail 2012; Hallen and Trail 2008). Therefore, we speculated that a defect in the turgor pressure of generation in Δ*Fgbzip16* might result in the defect of ascospore discharge. To test this hypothesis, we measured the concentrations of various ions and polyols in the asci of Δ*Fgbzip16*. The results showed that the concentrations of ions (K^+, Cl^-, Ca^{2+}, and Na^+) and polyols (glycerol, arabitol, mannitol, and glucose) were significantly lower in Δ*Fgbzip16* than PH-1 (Fig. 4b, c). These findings indicated that Δ*Fgbzip16* fails to discharge ascospores, which is attributed to the low turgor pressure in the asci. Therefore, FgBzip16 positively modulates ascospore discharge in *F. graminearum*.

RNA-seq analysis of the Δ*Fgbzip16* mutant

To elucidate the mechanisms by which FgBzip16 regulates ascospore discharge, RNA-seq analysis was performed using RNA isolated from the 8-day perithecia sample. Compared with the wild-type PH-1, 106 and 443 genes were upregulated and downregulated, respectively (Fig. 5a). As FgBzip16 plays a role in ascospore discharge, we subjected the differentially expressed genes (DEGs) to KEGG enrichment analysis. The major downregulated DEGs were related to fatty acid degradation, taurine and hypotaurine metabolism, ascorbate and aldarate metabolism, and fatty acids metabolism (Fig. 5b). These findings suggest that the deletion of *FgBZIP16* results in the downregulation of fatty acid metabolism and cellular differentiation. Moreover, some of the downregulated DEGs belonged to the fusarubin/bostrycoidin biosynthetic gene cluster, which is associated with perithecial pigmentation. KEGG pathway analyses revealed a decrease in the metabolism of fatty acids in Δ*Fgbzip16*. Notably, the deletion of *FgBZIP16* resulted in the downregulation of many genes related to fatty acid metabolism (Fig. 5b). In contrast, the genes involved in pyruvate metabolism were upregulated. Taken together, these results demonstrate that FgBzip16 positively regulates fatty acid metabolism during sexual development.

FgBzip16 targets fatty acid metabolism-related genes

As noted earlier, the discharge of ascospores is caused by the turgor pressure of the asci, which is generated by fatty acid metabolism. Through the analysis of RNA-Seq data, we found that two fatty acid metabolism-related genes (*FGSG_05321* and *FGSG_03244*) were differentially expressed (greater than two-fold). To explore the function of FgBzip16 in fatty acid metabolism, we first examined the relationship between FgBzip16, *FGSG_05321*, and *FGSG_03244* using an electrophoretic mobility shift assay (EMSA). The results showed that FgBzip16 binds to the putative promoter region 1500 bp upstream of

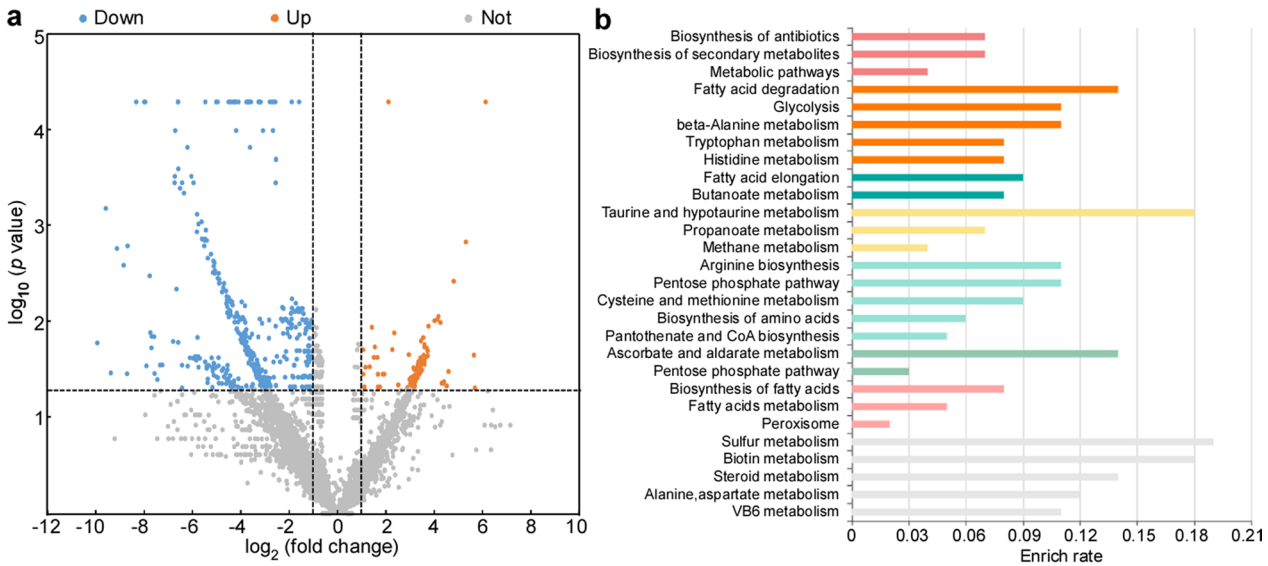

Fig. 5 RNA-Seq-based transcriptome analysis. **a** Analysis of differentially expressed genes showed significant increased (blue dots) and decreased (orange dots) in their expression, with over two-fold in the Δ*Fgbzip16* mutant in comparison with the wild- type strain PH-1. **b** KEGG enrichment analysis of the differentially expressed genes

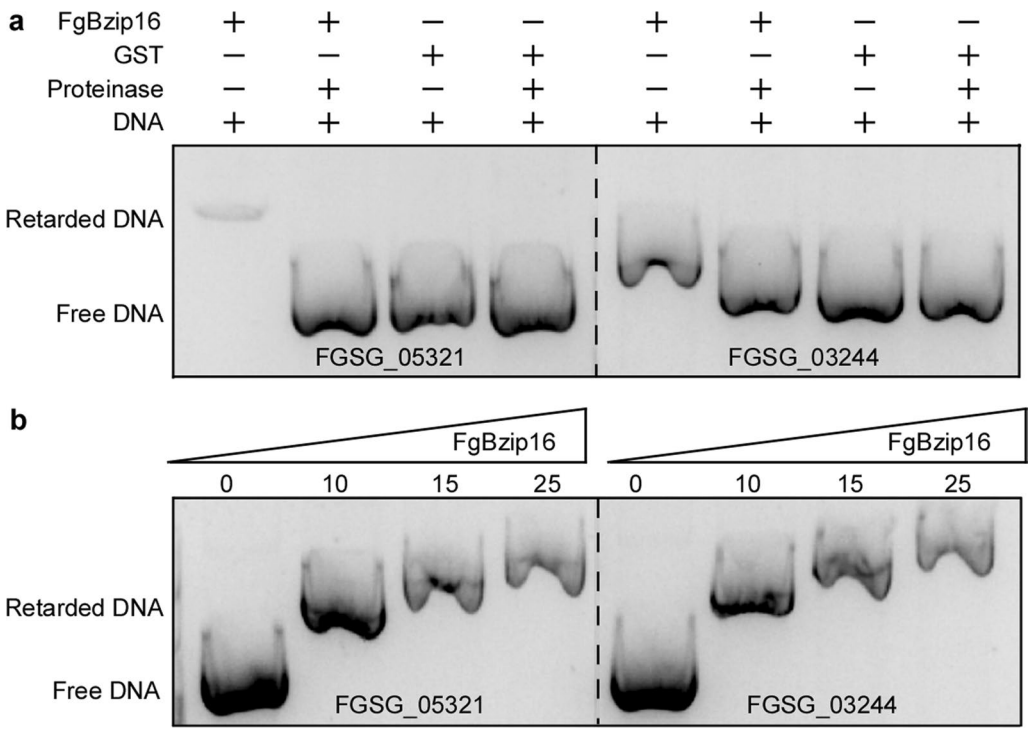

Fig. 6 FgBzip16 targets fatty acid biosynthesis and metabolism-related genes. **a** EMSA assays for the binding of FgBzip16 protein with putative promoter sequences of *FGSG_05321* and *FGSG_03244*, respectively. The 1500 bp DNA fragment of the putative promoter sequence of each gene was incubated in the absence or presence of purified FgBzip16 protein. GST protein or proteinase K was added after the incubation of FgBzip16 protein with DNA fragment as control. DNA–protein complexes were separated by 1.5% agarose gel electrophoresis and photographed. **b** EMSA assays with a gradient concentration of FgBzip16 protein

Table 2 Expression changes of the genes involved in fatty acid biosynthesis and metabolism in *F. graminearum FgBZIP16* deletion mutant by quantitative real-time PCR

Pathway	Accession number	Putative function	Fold change in gene expression[a]
Fatty acid biosynthesis	FGSG_05322	fatty acid synthase subunit beta dehydratase	0.692*
	FGSG_05321	fatty acid synthase subunit alpha reductase	0.191*
	FGSG_07226	3-oxoacyl-[acyl-carrier-protein] synthase, mitochondrial precursor	1.483*
	FGSG_02324	hypothetical protein similar to type I polyketide synthase	14.914*
	FGSG_02210	conserved hypothetical protein	0.431*
	FGSG_07223	hypothetical protein similar to short chain dehydrogenase family protein	1.016
	FGSG_03838	conserved hypothetical protein	0.711*
	FGSG_01857	hypothetical protein similar to 3-oxoacyl-acyl-carrier-protein reductase	1.547*
	FGSG_08816	conserved hypothetical protein	0.286*
	FGSG_11409	conserved hypothetical protein	0.034*
Fatty acid metabolism	FGSG_01419	hypothetical protein similar to AMP-binding protein	5.325*
	FGSG_13860	conserved hypothetical protein	3.638*
	FGSG_02287	hypothetical protein similar to acyl-CoA oxidase	10.254*
	FGSG_12573	hypothetical protein similar to enoyl-CoA hydratase/isomerase family protein	4.344*
	FGSG_05551	hypothetical protein similar to peroxisomal D3,D2-enoyl-CoA isomerase	1.442*
	FGSG_07659	hypothetical protein similar to fadD36	0.780*
	FGSG_03244	hypothetical protein similar to enoyl-CoA hydratase/isomerase family protein	15.687*
	FGSG_01581	conserved hypothetical protein	2.536*
	FGSG_03546	hypothetical protein similar to dehydrogenase	6.692*
	FGSG_13111	enoyl-CoA hydratase, mitochondrial precursor	1.634*

[a] Fold-change value represents the fold expression in *FgBZIP16* deletion mutant Δ*Fgbzip16* as compared with that in the wild-type strain PH-1. The asterisks indicate a significant difference, at $P < 0.01$

the start codon of these two genes. FgBzip16-DNA complexes migrated slower than the DNA fragments alone in an agarose gel without proteinase K treatment (Fig. 6a, b). We also investigated the expression of these two genes. RT-qPCR analysis revealed that the *FGSG_05321* decreased sharply in the Δ*Fgbzip16* mutant but not in the wild-type strain PH-1 (Table 2). *FGSG_03244* expression was significantly increased in Δ*Fgbzip16* than PH-1 (Table 2). These results suggest that FgBzip16 binds to the putative promoter regions of *FGSG_05321* and *FGSG_03244* and regulates their transcription.

FgBzip16 positively regulates fatty acid metabolism during sexual development

Transcriptome analysis reveals that FgBzip16 may positively modulate fatty acid metabolism, which is important for ascospore discharge. To confirm this result, we used Nile red staining to examine the distribution of lipid bodies of PH-1 and Δ*Fgbzip16*. In comparison to the wild type, a lower number of lipid bodies were detected in the Δ*Fgbzip16* mutant (Fig. 7a, b). In addition, we measured the concentration of glycerol and found a significant decrease in Δ*Fgbzip16* (Fig. 7c). To clarify the involvement of FgBzip16 in fatty acid metabolism-related genes during ascospore discharge, we compared fatty acid production between the wild-type and Δ*Fgbzip16* strains. Δ*Fgbzip16* had a significant decrease in fatty acid production than PH-1, especially in the early stage of sexual development (Fig. 7d). We further analyzed 20 genes that are associated with fatty acid biosynthesis and metabolism in *F. graminearum* and found that six out of the ten genes related to fatty acid biosynthesis were downregulated in the Δ*Fgbzip16* mutant, while eight out of the ten genes related to fatty acid metabolism were upregulated (Table 2). These results indicate that FgBzip16 is a positive regulator of fatty acid metabolism during sexual development.

Discussion

Sexual reproduction is a key factor in maintaining genetic diversity and stability in fungi. Ascospores play a crucial role in the spread of FHB disease (Zeller et al. 2004; Lee et al. 2009a, b). However, research on sexual reproduction in filamentous fungi, particularly in *F. graminearum*, is limited. In this study, we focused on b-ZIP TFs, which regulate various biological processes in eukaryotes. We identified and characterized *FgBZIP16* as a basic leucine zipper (b-ZIP) TF in *F. graminearum* and demonstrated that FgBzip16 functions as a TF that modulates fatty acid metabolism,

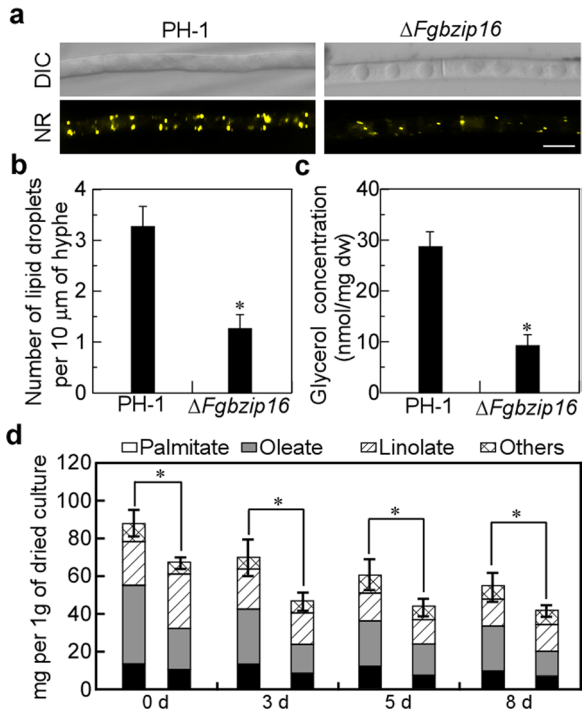

Fig. 7 Lipid accumulation in mycelia of *F. graminearum* strains. **a** Lipid accumulation of the indicated strains. Hyphae were stained with Nile red. Photographs were examined under differential interference contrast (DIC) or epifluorescence microscopy. Bar = 10 μm. **b** Statistical analysis of the number lipid droplets in **a**. Line bars in each column denote the standard errors of three repeated experiments. The asterisks indicate a significant difference, at $P < 0.01$. **c** The concentration of glycerol in hyphae of the indicated strains, respectively. Line bars in each column denote the standard errors of three repeated experiments. The asterisks indicate a significant difference at $P < 0.01$. **d** Fatty acids composition in perithecia of indicate strains. Line bars represent standard deviations of total lipid content (n = 3). Asterisks represent significant differences in the total lipid content between wild-type and Δ*Fgbzip16* mutant ($P < 0.01$)

controlling hyphal growth, conidia, ascospore discharge, and pathogenicity. This study provides a regulatory mechanism by which FgBzip16 is required for the infection-related morphogenesis and pathogenicity of FHB.

FgBzip16-mediated transcriptional regulation plays a crucial role not only in fungal development (growth and conidia) but also in the pathogenicity of *F. graminearum*. The RT-qPCR results showed that *FgBZIP16* was expressed at all development stages, including vegetative growth, conidiation, plant infection, and perithecia (Additional file 1: Figure S1). As a regulator, FgBzip16 appeared to play a role in various processes by activating downstream target genes (Fig. 8). The RNA-seq results also indicate that a few DEGs were related to growth and sexual development, showing that FgBzip16 is involved in various molecular processes depending on the developmental stage. Further studies are required to clarify the association between lipid metabolism and ascospore discharge controlled by FgBzip16 in *F. graminearum*.

Fatty acid metabolism is involved in many cellular functions, especially in generating energy for metabolic processes within cells (et al. 2007; Rajvanshi et al. 2017). Lipid metabolism is the principal route for fatty acid metabolism and is vital for the maintenance of cellular turgor pressure because lipids in excess are toxic to cells (Goepfert et al. 2005; et al. 2007). Furthermore, defects in lipid metabolism can lead to defective sexual reproduction (Shin et al. 2020; Tang et al. 2021; Zhang et al. 2021). Consistent with these findings, our data showed that the deletion of *FgBZIP16* resulted in defects in lipid metabolism, and the mutants were unable to discharge ascospores. Therefore, we conclude that FgBzip16 plays a crucial role in maintaining cellular turgor pressure during sexual reproduction. Our findings provide comprehensive insights into the basis of sexual reproduction in *F. graminearum*.

In this study, we found that the deletion of *FgBZIP16* altered morphogenesis and vegetative growth, and abolished the pathogenicity of *F. graminearum*. It is possible that the reduction in the growth rate of Δ*Fgbzip16* could be attributed to defects in plant infection. However, it is also likely that other crucial virulence factors were affected due to the complete loss of pathogenicity in the Δ*Fgbzip16* mutant. Previous research has shown that DON functions as a virulence factor that promotes wheat infection by *F. graminearum*. Nevertheless, our findings revealed that the concentration of DON remained unchanged in both the wild-type PH-1 and Δ*Fgbzip16* mutant strains, and RT-qPCR assays showed that the expression of the trichothecene synthase genes *TRI5* and *TRI6* did not change. Fungi can release a range of cell wall degrading enzymes during the infection of *F. graminearum* (Jenczmionka et al. 2003; Jenczmionka and Schafer 2005; Voigt et al. 2005). It is plausible that the reduced extracellular enzyme activity could also account for the loss of pathogenicity in the Δ*Fgbzip16* mutant. The endoglucanase activity was significantly reduced in the Δ*Fgbzip16*, which failed to penetrate cellophane or plants.

According to the massive phenotypic data of *F. graminearum*, key regulators such as TFs, vesicle trafficking, and kinases have been identified. These regulators can coordinate various environmental signals and are associated with fungal development and pathogenicity (Son et al. 2011; Yun et al. 2015; Li et al. 2019a). Some regulators possess global modulates, such as FgVelb,

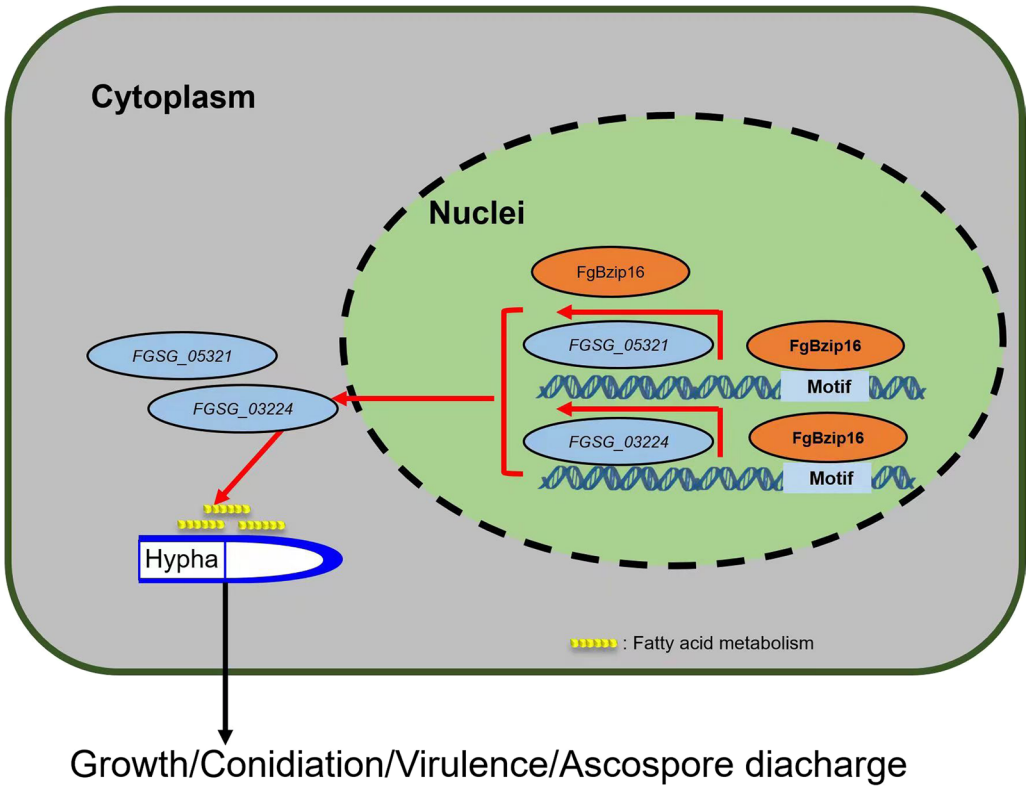

Fig. 8 A hypothetical model for FgBzip16 function in *F. graminearum*. Activation of FgBzip16 mediates the reprogramming of fatty acid metabolisms required for development, virulence, conidial and ascospore discharge

FgVeA, FgTri6, and FgLaeA, which are involved in developmental processes, and primary and secondary metabolism (Jiang et al. 2011, 2012; Nasmith et al. 2011; Kim et al. 2013), while others possess unique functions, such as sexual reproduction-related *MAT* genes, which are specifically involved in sexual development (Lee et al. 2003). In this study, we characterized the b-Zip factor FgBzip16, which is a regulator of fatty acid metabolism during sexual development. The regulatory pathways and networks involving FgBzip16 in *F. graminearum* remain unclear.

In conclusion, we have uncovered a regulatory mechanism whereby the b-Zip factor FgBzip16 acts as a positive regulator during the sexual development of the ascomycete fungus *F. graminearum*. FgBzip16 reprograms fatty acid metabolism and regulates vegetative growth, conidia and plant infections. This is the first reported highlighting the shared and specific functions associated with b-Zip transcription factor FgBzip16 and linking the regulatory roles to the fungal development, fatty acid metabolism, host penetration, and pathogenicity of *F. graminearum*.

Conclusions

In the present study, we identified and characterized the functions of *FgBZIP16* in *F. graminearum*. *FgBZIP16*, a basic leucine zipper (b-Zip) TF, acts as a transcriptional regulator of ascospore discharge. Targeted gene deletion revealed that FgBzip16 is important for vegetative growth, asexual/sexual development, and plant infection. Cytological observations have shown that FgBzip16 localized to the nucleus during the hyphal and conidial stages. Further investigation has revealed that FgBzip16 is required for ascospore discharge. By combining transcriptomics and molecular biology, we demonstrated that FgBzip16 binds to the promoter of its target genes, *FGSG_05321* (encoding fatty acid synthase subunit alpha reductase) and *FGSG_03244* (encoding enoyl hydratase), which regulate ascospore discharge of *F. graminearum*.

Methods

Strains and culture conditions

The wild-type *F. graminearum* strain PH-1 was used as the original strain for the transformation experiment. All strains were cultured on potato dextrose agar (PDA) medium (Li et al. 2019a). Liquid YEPD medium was used to prepare the mycelia for DNA and RNA extraction as

previously described (Li et al. 2019b, 2019c). For vegetative growth assay, 3 mm × 3 mm agar blocks were placed into PDA and CM plate at 28°C for 3 days (Li et al. 2019a). For sexual reproduction assays, the aerial hyphae of the indicated strains of 10-day-old carrot agar cultures were pressed down with 1 mL of sterile 0.1% Tween 20 as described (Li et al. 2019a).

Gene deletion and complementation

Gene deletion mutants were constructed using a split-marker PCR strategy (Zhang et al. 2016). The flanking sequence (approximately 1 kb) upstream and downstream of the *FgBZIP16* gene, and *HPH* cassette were amplified using primers in PCR. The 3.4-kb fragment was transformed into the protoplasts of wild-type PH-1, as previously described (Li et al. 2019b). To obtain the complemented strain, the fragment containing the entire *FgBZIP16* gene and GFP-tag, and then inserted into the pYF11 plasmid using the yeast gap repair approach (Li et al. 2017). The resulting constructs were sequenced and transformed into the Δ*Fgbzip16* mutant. The complemented transformants were screened by GFP signal under a fluorescence microscope. The primers are also listed in Supplementary Information (Additional file 2: Table S1).

Pathogenicity and DON assays

Pathogenicity was performed on flowering wheat inflorescences as previously described with minor modifications (Zhang et al. 2016; Li et al. 2019a). Approximately 6-week-old flowering wheat heads were infected with 1×10^5 spores/mL and 10 µL of each. 10 µL water served as controls. After two weeks, we analyzed the typical head blight symptoms. For each treatment, thirty wheat heads were inoculated. The hyphal colonization on infected wheat spikelets was observed using a Hitachi TM-1000 tabletop microscope (Li et al. 2018).

For DON production assays, five mycelial plugs of each strain were inoculated with 50 g healthy and autoclaved wheat kernels as previously described (Li et al. 2018). The wheat kernels were inoculated at 28°C for 20 days. DON was extracted according to the manufacturer's recommendations protocol with minor modifications (Li et al. 2019a), and subsequently further purified PuriTox SR DON columnTC-T200 (Trilogy an- alytical laboratory). To determine the DON and fungal ergosterol using an HPLC system Waters 1525 (Waters Co., Massachusetts, USA). The experiment was repeated three times.

Staining and confocal microscopy

F. graminearum cells, including hyphae and conidia expressing green fluorescent fusion proteins, were incubated under appropriate conditions. Epifluorescence microscopy was observed under a confocal fluorescence microscope (LSM710, 63 × oil; Zeiss). To examine nuclei, hyphae, and conidia were stained with 4′, 6-diamidino-2-phenylindole (DAPI) (Molecular Probes, Eugene, OR, USA) at a concentration of 1 mg/mL at room temperature in darkness for 5 min (Feng et al. 2021). For lipid droplet staining, hyphae were stained with BODIPY™ 493/503 (final concentration of 1 mg/mL) and incubation at the room temperature for 3 min (Rajvanshi et al. 2017; Liu et al. 2009). Photographs were taken using confocal fluorescence microscopy, as described earlier.

Ascospore discharge assays

For ascospore discharge as previously described with minor modifications (Li et al. 2019a). Mycelial plugs with perithecia were placed on the end of a glass slide, and the surface of the glass slide was perpendicular to the perithecia-bearing surface. Inoculated slides were kept in a platform at 28°C with 90% humidity and in the dark for 24 h, followed by a 12 h/12 h light/dark. Photographs were taken using a Hitachi TM-1000 tabletop microscope.

Ions and polyols concentration assays

The concentrations of K^+, Ca^{2+}, and Na^+ were determined as previously described (Almeida et al. 2015; Yang et al. 2018) with minor modifications. The perithecia of the indicated strains were harvested, dried using a freeze drier, and digested with a solution containing 98% H_2SO_4. Subsequently, 30% H_2O_2 was added to restore the colorless, perithecia digestion solution. Next, the digestion was measured using a flame spectrophotometer (TAS-986F, Beijing Purkinje General Instrument Co. Ltd., China). The Cl^- concentrations were assayed by spectrophotometry following the chloride kit instructions (MAK023, Sigma-Aldrich) using a spectrophotometer (620 nm). The experiments were performed in triplicates. Glycero, mannitol, and glucose concentrations assays were performed using the kit instructions (MAK117, Sigma-Aldrich; MAK096, Sigma-Aldrich; MAK263, Sigma-Aldrich), with modifications. Arabitol content was determined using an HPLC system Waters 1525 (Waters Co., Massachusetts, USA). The experiment was repeated three times.

Endoglucanase activity assay

In order to ensure a comparable physiological status and biomass of the inoculum, the conidia were recultivated in CM medium (containing 0.05% yeast extract, 1% glucose, and 1 × yeast nitrogen base) at room temperature for 4 days as described previously (Li et al. 2018, 2019a). Then the mycelia were isolated by filtration, washed using sterile water and used to inoculate 100 mL of induction

medium (containing mineral salts and trace elements). 0.2 mg/mL casein and 0.5% CMC sodium salt as the sole carbon sources were added individually, and the mycelia-induced cultures were collected at 24 h after inoculation. The culture supernatant was isolated by centrifugation for 10 min at maximum speed (Jenczmionka and Schafer 2005). Endoglucanase activity was determined using carboxymethylcellulose as the sole carbon source and substrate for the enzyme assay. Under this condition, endoglucanase activity is specifically assayed. 30 µL culture supernatant was added to 270 µL of substrate solution (1% CMC sodium salt, dissolved in 50 mM sodium acetate, pH 5.0) and incubated at 37°C. The reducing sugars were examined by a spectrophotometric assay (Waffenschmidt and Jaenicke 1987). Calibration curves were made from standard glucose solutions. Reducing 1 nmol/min sugars released from the substrate as one unit of enzymatic activity.

Quantification of gene expression by RT-qPCR

Total RNA samples were extracted from mycelia, conidia, and perithecia using an RNA extraction kit (Vazyme Biotech, Nanjing, China) according to the manufacturer's protocol. cDNA was prepared using reverse transcriptase HiScript III RT SuperMix for qPCR (Vazyme Biotech, Nanjing, China). Quantitative PCR was run on a Real-time PCR system (Eppendorf) with ChamQ SYBR® qPCR Mix (Q311-02, Vazyme Biotech). The relative quantification of each transcript was calculated by the $2^{-\Delta\Delta CT}$ method. The primers used in this section are listed in Additional file 2: Table S1.

RNA-seq and bioinformatics analysis

Perithecia of PH-1 and ΔFg*bzip16* mutants were harvested at 10 days from the carrot agar plate and used for RNA extraction with TRIzol (Invitrogen, USA). RNA-Seq libraries were constructed using the Illumina TruSeq™ RNA Sample Preparation Kit (Illumina, San Diego, CA, USA) according to the manufacturer's protocol. Samples were run on an Illumina HiSeq2000 instrument using the reagents provided in the Illumina TruSeq Paired-End (PE) Cluster Kit V3-cBot-HS and the TruSeq SBS kit v3-HS.

Relative transcript abundance was measured in reads per kilobase of exon per million mapped sequence reads (RPKM) (Mortazavi et al. 2008). The differentially expressed genes ($\log_2$FC > 1 and FDR < 0.05) were carried out based on the reads counts by edgeRun with TMM normalization as described previously (Dimont et al. 2015). KEGG pathway analysis using the website (https://www.kegg.jp/kegg/) (Ruepp et al. 2004; Supek et al. 2011).

EMSA assays

The cDNA of FgBzip16 was cloned into the pGEX-4 T-2 vector to express GST-tagged *FgBZIP16* heterogeneously. FgBzip16 protein expressed in *Escherichia coli* BL21-CodonPlus (DE3) cells (Sigma-Aldric, CMC0014) was separated and purified using a Ni–NTA agarose (QIAGEN, Germany) according to the manufacturer's instruction book. The DNA fragment of the putative gene promoter was amplified by PCR using the primers (Additional file 2: Table S1), mixed with the purified FgBzip16 protein and incubated for 20 min at 25°C, and then separated by agarose gel electrophoresis. Gels were visualized directly using a BIO-RAD scanner.

Accession number

The gene sequences can be found using the following accession number at the website (http://eupathdb.org/eupathdb/): *FgBZIP16* (FGSG_09832).

Statistical analysis

All experiments were repeated at least three replicates. Significant differences between treatments were evaluated using SPSS software (version 2.0). The data for two different treatments were compared statistically using ANOVA, followed by an *F*-test if the ANOVA result was significant at $P < 0.01$.

Abbreviations

BLASTP	Protein basic local alignment search tool
bZIP	Basic leucine zipper
DEGs	Differentially expressed genes
DON	Deoxynivalenol
EMSA	Electrophoretic mobility shift assay
FHB	Fusarium head blight
PDA	Potato dextrose agar
PEX	Peroxins
RT-qPCR	Real time quantitative polymerase chain reaction
TFs	Transcription factors
YEPD	Yeast extract peptone dextrose
ZEA	Zearalenone

Supplementary Information

The online version contains supplementary material available at https://doi.org/10.1186/s42483-023-00190-0.

Additional file 1. Figure S1. The structural domains and expression profiles of *FgBZIP16*. a Schematic drawing of the conserved domains in FgBzip16. FgBzip16 has a b-zip domain (marked as a black box, 152-219 aa) at the N-terminal region. b The expression of *FgBZIP16* was measured by quantitative real-time RT-PCR with cDNA from samplings for hyphae, conidia, infected wheat heads (infected wheat) and perithecium. The relative abundance of *FgBZIP16* transcripts during infectious was normalized by comparing with hyphae in liquid CM (arbitrarily set to 1). Each sample was harvested from 10 plants and three independent experiments, each with three replicates, were performed. Line bars in each column denote the standard errors of three repeated experiments. The asterisks indicate a significant difference at $P < 0.01$. **Figure S2**. Targeted gene replacement of *FgBZIP16* in *F. graminearum*. a Schematic diagram of the split-marker gene deletion strategy for *FgBZIP16*. b Results from Southern blot analysis of

genomic DNA using gene-specific or *HPH* probes. DNA from the mutant hybridizes only to the *HPH* probe, while that from the wild type hybridizes only to the gene-specific probe. **Figure S3**. Deoxynivalenol (DON) production and the expression of DON biosynthesis genes. a DON production measurement in infected wheat kernels 20 days. Line bars in each column denote the standard errors of three repeated experiments. The asterisks indicate a significant difference at $P < 0.01$. b RT-qPCR analyzes the relative transcription abundance of trichothecene synthase genes *TRI5* and *TRI6*. Line bars in each column denote the standard errors of three repeated experiments. The asterisks indicate a significant difference at $P < 0.01$.

Additional file 2. Table S1. Primers were used in this study.

Acknowledgements
Not applicable.

Author contributions
BL and WY designed research; BL, YS, and LY performed experiments; HS, YZ, and KC contributed new reagents/analytical tools; RM, JL, and WY analyzed data; and BL and ZJ wrote the manuscript. All authors read and approved the final manuscript.

Funding
This study was supported by the National Natural Science Foundation of China (Grant No: 32101530), the Natural Science Foundation of Jiangsu Province (Grant No: BK20200953), the Open Project of State Key Laboratory for Biology of Plant Diseases and Insect Pests (Grant No: SKLOF 202202), the Foundation of Key Technology Research Project of Henan Province (Grant No: 222102110031), and the China Postdoctoral Science Foundation (Grant No: 2022M712886).

Availability of data and materials
Not applicable.

Declarations

Ethics approval and consent to participate
Not applicable.

Consent for publication
Not applicable.

Competing interests
The authors declare that they have no competing interests.

Received: 6 February 2023 Accepted: 23 July 2023
Published online: 21 August 2023

References

Almeida SM, Umeo SH, Marcante RC, Yokota ME, Valle JS, Dragunski DC, et al. Iron bioaccumulation in mycelium of *Pleurotus ostreatus.* Braz J Microbiol. 2015; 46(1):195–200. https://doi.org/10.1590/S1517838246120130695

Audenaert K, Vanheule A, Hofte M, Haesaert G. Deoxynivalenol: a major player in the multifaceted response of *Fusarium* to its environment. Toxins (basel). 2013;6(1):1–19. https://doi.org/10.3390/toxins6010001.

Bai G, Shaner G. Management and resistance in wheat and barley to fusarium head blight. Annu Rev Phytopathol. 2004;42:135–61. https://doi.org/10.1146/annurev.phyto.42.040803.140340.

Boisnard S, Espagne E, Zickler D, Bourdais A, Riquet AL, Berteaux-Lecellier V. Peroxisomal ABC transporters and beta-oxidation during the life cycle of the filamentous fungus *Podospora anserina*. Fungal Genet Biol. 2009;46(1):55–66. https://doi.org/10.1016/j.fgb.2008.10.006.

Calvo AM, Gardner HW, Keller NP. Genetic connection between fatty acid metabolism and sporulation in *Aspergillus nidulans*. J Biol Chem. 2001;276(28):25766–74. https://doi.org/10.1074/jbc.M100732200.

Cavinder B, Trail F. Role of Fig1, a component of the low-affinity calcium uptake system, in growth and sexual development of filamentous fungi. Eukaryot Cell. 2012;11(8):978–88. https://doi.org/10.1128/EC.00007-12.

Cavinder B, Sikhakolli U, Fellows KM, Trail F. Sexual development and ascospore discharge in *Fusarium graminearum*. J vis Exp. 2012;61:3895. https://doi.org/10.3791/3895.

Dimont E, Shi J, Kirchner R, Hide W. edgeRun: an R package for sensitive, functionally relevant differential expression discovery using an unconditional exact test. Bioinformatics. 2015;31(15):2589–90. https://doi.org/10.1093/bioinformatics/btv209.

Feng W, Yin Z, Wu H, Liu P, Liu X, Liu M, et al. Balancing of the mitotic exit network and cell wall integrity signaling governs the development and pathogenicity in *Magnaporthe oryzae*. PLoS Pathog. 2021;17(1):e1009080. https://doi.org/10.1371/journal.ppat.1009080.

Goepfert S, Vidoudez C, Rezzonico E, Hiltunen JK, Poirier Y. Molecular identification and characterization of the *Arabidopsis* delta (3,5), delta(2,4)-dienoyl-coenzyme A isomerase, a peroxisomal enzyme participating in the beta-oxidation cycle of unsaturated fatty acids. Plant Physiol. 2005;138(4):1947–56. https://doi.org/10.1104/pp.105.064311.

Goswami RS, Kistler HC. Heading for disaster: *Fusarium graminearum* on cereal crops. Mol Plant Pathol. 2004;5(6):515–25. https://doi.org/10.1111/j.1364-3703.2004.00252.x.

Gu Q, Chen Y, Liu Y, Zhang C, Ma Z. The transmembrane protein FgSho1 regulates fungal development and pathogenicity via the MAPK module Ste50-Ste11-Ste7 in *Fusarium graminearum*. New Phytol. 2015;206(1):315–28. https://doi.org/10.1111/nph.13158.

Guenther JC, Trail F. The development and differentiation of Gibberella zeae (anamorph: *Fusarium graminearum*) during colonization of wheat. Mycologia. 2005;97(1):229–37. https://doi.org/10.3852/mycologia.97.1.229.

Hallen HE, Trail F. The L-type calcium ion channel cch1 affects ascospore discharge and mycelial growth in the filamentous fungus *Gibberella zeae* (anamorph *Fusarium graminearum*). Eukaryot Cell. 2008;7(2):415–24. https://doi.org/10.1128/EC.00248-07.

Hynes MJ, Murray SL, Khew GS, Davis MA. Genetic analysis of the role of peroxisomes in the utilization of acetate and fatty acids in *Aspergillus nidulans*. Genetics. 2008;178(3):1355–69. https://doi.org/10.1534/genetics.107.085795.

Jansen C, Wettstein D, Schafer W, Kogel KH, Felk A, Maier FJ. Infection patterns in barley and wheat spikes inoculated with wild-type and trichodiene synthase gene disrupted *Fusarium graminearum*. Proc Natl Acad Sci U S A. 2005;102(46):16892–7. https://doi.org/10.1073/pnas.0508467102.

Jenczmionka NJ, Schafer W. The Gpmk1 MAP kinase of *Fusarium graminearum* regulates the induction of specific secreted enzymes. Curr Genet. 2005;47(1):29–36. https://doi.org/10.1007/s00294-004-0547-z.

Jenczmionka NJ, Maier FJ, Losch AP, Schafer W. Mating, conidiation and pathogenicity of *Fusarium graminearum*, the main causal agent of the head-blight disease of wheat, are regulated by the MAP kinase gpmk1. Curr Genet. 2003;43(2):87–95. https://doi.org/10.1007/s00294-003-0379-2.

Jiang J, Liu X, Yin Y, Ma Z. Involvement of a velvet protein FgVeA in the regulation of asexual development, lipid and secondary metabolisms and virulence in *Fusarium graminearum*. PLoS ONE. 2011;6(11):e28291. https://doi.org/10.1371/journal.pone.0028291.

Jiang J, Yun Y, Liu Y, Ma Z. *FgVELB* is associated with vegetative differentiation, secondary metabolism and virulence in *Fusarium graminearum*. Fungal Genet Bio. 2012;49(8):653–62. https://doi.org/10.1016/j.fgb.2012.06.005.

Kim HK, Lee S, Jo SM, McCormick SP, Butchko RA, Proctor RH, et al. Functional roles of FgLaeA in controlling secondary metabolism, sexual development, and virulence in *Fusarium graminearum*. PLoS ONE. 2013;8(7):e68441. https://doi.org/10.1371/journal.pone.0068441.

Lee J, Lee T, Lee YW, Yun SH, Turgeon BG. Shifting fungal reproductive mode by manipulation of mating type genes: obligatory heterothallism of *Gibberella zeae*. Mol Microbiol. 2003;50(1):145–52. https://doi.org/10.1046/j.1365-2958.2003.03694.x.

Lee J, Chang IY, Kim H, Yun SH, Leslie JF, Lee YW. Genetic diversity and fitness of *Fusarium graminearum* populations from rice in Korea. Appl Environ Microbiol. 2009a;75(10):3289–95. https://doi.org/10.1128/AEM.02287-08.

Lee SH, Han YK, Yun SH, Lee YW. Roles of the glyoxylate and methylcitrate cycles in sexual development and virulence in the cereal pathogen *Gibberella zeae*. Eukaryot Cell. 2009b;8(8):1155–64. https://doi.org/10.1128/EC.00335-08.

Li B, Liu L, Li Y, Dong X, Zhang H, Chen H, et al. The FgVps39-FgVam7-FgSso1 complex mediates vesicle trafficking and is important for the development and virulence of *Fusarium graminearum*. Mol Plant Microbe Interact. 2017;30(5):410–22. https://doi.org/10.1094/MPMI-11-16-0242-R.

Li B, Dong X, Li X, Chen H, Zhang H, Zheng X, et al. A subunit of the HOPS endocytic tethering complex, FgVps41, is important for fungal development and plant infection in *Fusarium graminearum*. Environ Microbiol. 2018;20(4):1436–51. https://doi.org/10.1111/1462-2920.14050.

Li B, Dong X, Zhao R, Kou R, Zheng X, Zhang H. The t-SNARE protein FgPep12, associated with FgVam7, is essential for ascospore discharge and plant infection by trafficking Ca^{2+} ATPase FgNeo1 between Golgi and endosome/vacuole in *Fusarium graminearum*. PLoS Pathog. 2019a;15(5):e1007754. https://doi.org/10.1371/journal.ppat.1007754.

Li B, Gao Y, Mao HY, Borkovich KA, Ouyang SQ. The SNARE protein FolVam7 mediates intracellular trafficking to regulate conidiogenesis and pathogenicity in *Fusarium oxysporum f. sp. lycopersici*. Environ Microbiol. 2019b;21(8):2696–706. https://doi.org/10.1111/1462-2920.14585.

Li B, Mao HY, Zhang ZY, Chen XJ, Ouyang SQ. FolVps9, a guanine nucleotide exchange factor for FolVps21, is essential for fungal development and pathogenicity in *Fusarium oxysporum f. sp. lycopersici*. Front Microbiol. 2019c;10:2658. https://doi.org/10.3389/fmicb.2019.02658.

Liu N, Yun Y, Yin Y, Hahn M, Ma Z, Chen Y. Lipid droplet biogenesis regulated by the FgNem1/Spo7-FgPah1 phosphatase cascade plays critical roles in fungal development and virulence in *Fusarium graminearum*. New Phytol. 2009;223(1):412–29. https://doi.org/10.1111/nph.15748.

Min K, Son H, Lee J, Choi GJ, Kim JC, LeeYW,. Peroxisome function is required for virulence and survival of *Fusarium graminearum*. Mol Plant Microbe Interact. 2012;25(12):1617–27. https://doi.org/10.1094/MPMI-06-12-0149-R.

Mortazavi A, Williams BA, McCue K, Schaeffer L, Wold B. Mapping and quantifying mammalian transcriptomes by RNA-Seq. Nat Methods. 2008;5(7):621–8. https://doi.org/10.1038/nmeth.1226.

Nasmith CG, Walkowiak S, Wang L, Leung WW, Gong Y, Johnston A, et al. Tri6 is a global transcription regulator in the phytopathogen *Fusarium graminearum*. PLoS Pathog. 2011;7(9):e1002266. https://doi.org/10.1371/journal.ppat.1002266.

Pabo CO, Sauer RT. Transcription factors: structural families and principles of DNA recognition. Annu Rev Biochem. 1992;61:1053–95. https://doi.org/10.1146/annurev.bi.61.070192.005201.

Paul PA, Lipps PE, Hershman DE, McMullen MP, Draper MA, Madden LV. Efficacy of triazole-based fungicides for fusarium head blight and deoxynivalenol control in wheat: a multivariate meta-analysis. Phytopathology. 2008;98(9):999–1011. https://doi.org/10.1094/PHYTO-98-9-0999.

Proctor RH, Hohn TM, McCormick SP. Reduced virulence of *Gibberella zeae* caused by disruption of a trichothecene toxin biosynthetic gene. Mol Plant Microbe Interact. 1995;8(4):593–601. https://doi.org/10.1094/mpmi-8-0593.

Rajvanshi PK, Arya M, Rajasekharan R. The stress-regulatory transcription factors Msn2 and Msn4 regulate fatty acid oxidation in budding yeast. J Biol Chem. 2017;292(45):18628–43. https://doi.org/10.1074/jbc.M117.801704.

Ruepp A, Zollner A, Maier D, Albermann K, Hani J, Mokrejs M, et al. Mewes, The FunCat, a functional annotation scheme for systematic classification of proteins from whole genomes. Nucleic Acids Res. 2004;32(18):5539–45. https://doi.org/10.1093/nar/gkh894.

Seong KY, Pasquali M, Zhou X, Song J, Hilburn K, McCormick S, et al. Global gene regulation by Fusarium transcription factors Tri6 and Tri10 reveals adaptations for toxin biosynthesis. Mol Microbiol. 2009;72(2):354–67. https://doi.org/10.1111/j.1365-2958.2009.

Shelest E. Transcription factors in fungi. FEMS Microbiol Lett. 2008;286(2):145–51. https://doi.org/10.1111/j.1574-6968.2008.01293.x.

Shin J, Bui DC, Kim S, Jung SY, Nam HJ, Lim JY, et al. The novel b-ZIP transcription factor Fpo1 negatively regulates perithecial development by modulating carbon metabolism in the ascomycete fungus *Fusarium graminearum*. Environ Microbiol. 2020;22(7):2596–612. https://doi.org/10.1111/1462-2920.14960.

Son H, Seo YS, Min K, Park AR, Lee J, Jin JM, et al. A phenome-based functional analysis of transcription factors in the cereal head blight fungus, *Fusarium graminearum*. PLoS Pathog. 2011;7(10):e1002310. https://doi.org/10.1371/journal.ppat.1002310.

Supek F, Bosnjak M, Skunca N, Smuc T. REVIGO summarizes and visualizes long lists of gene ontology terms. PLoS ONE. 2011;6(7):e21800. https://doi.org/10.1371/journal.pone.0021800.

Tang L, Chi H, Li W, Zhang L, Zhang L, Chen L, et al. FgPsd2, a phosphatidylserine decarboxylase of *Fusarium graminearum*, regulates development and virulence. Fungal Genet Biol. 2021;146:103483. https://doi.org/10.1016/j.fgb.2020.103483.

Trail F. Fungal cannons: explosive spore discharge in the *Ascomycota*. FEMS Microbiol Lett. 2007;276(1):12–8. https://doi.org/10.1111/j.1574-6968.2007.00900.x.

Trail F, Xu H, Loranger R, Gadoury D. Physiological and environmental aspects of ascospore discharge in *Gibberella zeae* (anamorph *Fusarium graminearum*). Mycologia. 2002;94(2):181–9. https://doi.org/10.2307/3761794.

Voigt CA, Schafer W, Salomon S. A secreted lipase of *Fusarium graminearum* is a virulence factor required for infection of cereals. Plant J. 2005;42(3):364–75. https://doi.org/10.1111/j.1365-313X.2005.02377.x.

Waffenschmidt S, Jaenicke L. Assay of reducing sugars in the nanomole range with 2,2′-bicinchoninate. Anal Biochem. 1987;165(2):337–40. https://doi.org/10.1016/0003-2697(87)90278-8.

Wang ZY, Soanes DM, Kershaw MJ, Talbot NJ. Functional analysis of lipid metabolism in *Magnaporthe grisea* reveals a requirement for peroxisomal fatty acid beta-oxidation during appressorium-mediated plant infection. Mol Plant Microbe Interact. 2007;20(5):475–91. https://doi.org/10.1094/MPMI-20-5-0475.

Wang L, Zhang L, Liu C, Sun S, Liu A, Liang Y, et al. The roles of FgPEX2 and FgPEX12 in virulence and lipid metabolism in *Fusarium graminearum*. Fungal Genet Biol. 2008;135:103288. https://doi.org/10.1016/j.fgb.2019.103288.

Yang JY, Fang YL, Wang P, Ye JR, Huang L. Pleiotropic roles of ChSat4 in asexual development, cell wall integrity maintenance, and pathogenicity in *Colletotrichum higginsianum*. Front Microbiol. 2018;9:2311. https://doi.org/10.3389/fmicb.2018.02311

Yun Y, Liu Z, Yin Y, Jiang J, Chen Y, Xu JR, et al. Functional analysis of the *Fusarium graminearum* phosphatome. New Phytol. 2015;207(1):119–34. https://doi.org/10.1111/nph.13374.

Zeller KA, Bowden RL, Leslie JF. Population differentiation and recombination in wheat scab populations of *Gibberella zeae* from the United States. Mol Ecol. 2004;13(3):563–71. https://doi.org/10.1046/j.1365-294x.2004.02098.x.

Zhang H, Li B, Fang Q, Li Y, Zheng X, Zhang Z. SNARE protein FgVam7 controls growth, asexual and sexual development, and plant infection in *Fusarium graminearum*. Mol Plant Pathol. 2016;17(1):108–19. https://doi.org/10.1111/mpp.12267.

Zhang L, Liu C, Wang M, Tao Y, Liang Y, Yu J. Peroxin FgPEX22-like is involved in FgPEX4 tethering and *Fusarium graminearum* pathogenicity. Front Microbiol. 2021;12:756292. https://doi.org/10.3389/fmicb.2021.756292.